Journal of Materials Chemistry C

RSC Publishing

PAPER

View Article Online
View Journal | View Issue

Cite this: *J. Mater. Chem. C*, 2013, **1**, 4640

A tetraphenylethene-substituted pyridinium salt with multiple functionalities: synthesis, stimuli-responsive emission, optical waveguide and specific mitochondrion imaging†

Na Zhao,[ab] Min Li,[ab] Yongli Yan,[c] Jacky W. Y. Lam,[ab] Yi Lin Zhang,[d] Yong Sheng Zhao,[c] Kam Sing Wong[d] and Ben Zhong Tang*[abe]

Received 23rd April 2013
Accepted 6th June 2013

DOI: 10.1039/c3tc30759j

www.rsc.org/MaterialsC

In this work, a heteroatom-containing luminogen (TPE-Py) with multi-functionalities was synthesized in a reasonable yield by melding a pyridinium unit with tetraphenylethene through vinyl functionality. TPE-Py is weakly emissive in solution but becomes a strong emitter when aggregated as nanoparticle suspensions in poor solvents or in the solid state, displaying a phenomenon of aggregation-induced emission. Crystallization generally weakens and red-shifts the light emission. The crystalline aggregates of TPE-Py, however, emit stronger and bluer light than their amorphous counterparts. The solid-state emission of TPE-Py can be reversibly switched between green and yellow color by grinding–fuming and grinding–heating processes with a high contrast due to the transformation from the crystalline to the amorphous state and *vice versa*. The large Stokes shift and well-ordered molecular arrangement of the crystalline microrods of TPE-Py make it promising as an optical waveguide material with a low optical loss coefficient of ~0.032 dB μm^{-1}. TPE-Py works as a good fluorescent visualizer for specific staining of mitochondria in living cells with a high photostability, thanks to its hydrophobic and cationic features.

Introduction

Development of new materials with advanced functionalities is a crucial step for future technological innovations. Luminescent materials have attracted much interest because of their wide applications in electronics,[1] optics,[2] storage media[3] and biological science.[4] Whereas luminescence behaviours of conjugated molecules and polymers are normally investigated in the solution state, they are utilized in the solid state (*e.g.*, as thin films) for real-world applications, where the luminophores tend to form aggregates. It is known that aggregation of organic luminophores often results in partial or even complete quenching of their light emission.[5] This effect of aggregation-caused quenching (ACQ) has limited the scope of their technological applications. We and other groups, however, observed a phenomenon of aggregation-induced emission (AIE) in some propeller-like molecules such as tetraphenylethene (TPE) and silole that is exact opposite to the ACQ effect.[6] Instead of quenching, aggregate formation has made these luminogens to emit efficiently though they are almost non-fluorescent in the solution state. Based on theoretical and experimental studies, the restriction of intramolecular rotation (RIR) is considered to be the main cause for the AIE phenomenon.[7] Since AIE luminogens are highly emissive in the aggregated state, this unique characteristic differentiates them from conventional luminophores and makes them promising materials for high-technological applications in the practically useful solid state.[8] As a result, various AIE dyes have been developed and their utilities in many fields such as organic light-emitting diodes,[9] bioprobes,[10] chemosensors[11] and cell imaging[12] have been explored, thanks to the enthusiastic efforts of the scientists.

Most of AIE dyes prepared so far show blue or green emission.[13] For biological scientists, they prefer luminogens with longer-wavelength emissions as these luminescent materials suffer little interferences from optical self-absorption and autofluorescence from the background.[14] For red-emissive dyes,

[a]*HKUST-Shenzhen Research Institute, No. 9 Yuexing 1st RD, South Area, Hi-tech Park, Nanshan, Shenzhen, 518057, China. E-mail: tangbenz@ust.hk*

[b]*Department of Chemistry, Institute for Advanced Study, Institute of Molecular Functional Materials and Division of Biomedical Engineering, The Hong Kong University of Science & Technology (HKUST), Clear Water Bay, Kowloon, Hong Kong, China*

[c]*CAS Key Laboratory of Photochemistry, Beijing National Laboratory for Molecular Science, Institute of Chemistry, Chinese Academy of Sciences, Beijing, 100190, P. R. China*

[d]*Department of Physics, HKUST, Clear Water Bay, Kowloon, Hong Kong, China*

[e]*Guangdong Innovative Research Team, SCUT-HKUST Joint Research Laboratory, State Key Laboratory of Luminescent Materials and Device, South China University of Technology, Guangzhou, 51640, China*

† Electronic supplementary information (ESI) available: Experimental section, UV-vis and PL emission spectra, TEM image and ED pattern, and bright-field and fluorescent images of living cells. See DOI: 10.1039/c3tc30759j

they are generally constructed from merged planar rings with extended conjugation or possess a strong intramolecular charge transfer (ICT) effect caused by the interaction between the electron-donating and accepting groups.[15] However, it is synthetically difficult to prepare luminogens with highly conjugated structures, while materials with the ICT feature can offer only weak emissions, particularly in a polar medium.[16] Recently, we succeeded in synthesizing a red-emissive luminogen by melding a benzothiazolium unit with TPE.[17] Although the hybrid molecule exhibits the ICT characteristic, it emits intensely in the aggregated or solid state due to the prevailed AIE effect contributed by the TPE unit. Such a result shows that the synergy interplay between the ICT and AIE attributes has led to efficient solid-state emitters with emissions at the longer wavelengths. On the other hand, many AIE dyes prepared previously are based on their potential utility in a specific single aspect such as organic light-emitting diodes or fluorescent sensors.[9b,11a] Few of them, however, exhibit multi-functionality or purpose.[18] Thus, development of efficient luminescent materials in the solid state with potential high-tech applications in various fields through a simple synthetic procedure is of interest from the concept of convenience and efficiency in the modern society. Furthermore, few AIE molecules can stain the organelles, especially mitochondrion, which is an important organelle in living cells,[12a] although many of them work as good fluorescent visualizers for cytoplasmic imaging.[12b,c]

Based on the strategy discussed above, in this paper, we report the synthesis of a new yellow-emissive AIE dye (TPE-Py, Scheme 1) by attaching a pyridinium unit to TPE through vinyl functionality, and present its multi-functional properties including morpho- and mechano-chromism, optical waveguide and mitochondrion imaging, which are extraordinary, if not unprecedented.

Results and discussion

Synthesis and optical property

TPE-Py was synthesized according to the synthetic route shown in Scheme 1.[17] 1,4-Dimethylpyridinium iodide (**1**) and 4-(1,2,3-triphenylvinyl)benzaldehyde (**2**) were prepared by the synthetic procedures as shown in Scheme S1 in the ESI† and heated under reflux in ethanol, which gave TPE-Py in a reasonable yield after counter anion exchange and purification by column chromatography. Detailed information on their synthesis and characterization data can be found in the ESI.†

The dilute THF solution (20 μM) of TPE-Py exhibits an absorption maximum at 403 nm (Fig. S1†). Photoexcitation of the solution induces a weak red emission at 625 nm, giving a Stokes shift as large as 222 nm (Fig. S1†). The fluorescence quantum yield (Φ_F) estimated using coumarin 153 (Φ_F = 58% in ethanol) is merely 3.5%, suggesting that TPE-Py is a weak emitter in the solution state. When the measurements are carried out in other solvents with increasing polarity, the emission spectrum moves to the longer-wavelength region accompanying with a decrease in the emission intensity (Fig. S2†), which is demonstrative of an ICT effect caused by the interaction between the electron-donating TPE unit and the electron-accepting pyridinium moiety.[4] The emission was weakened progressively when up to 90% water was added to the THF solution but started to swiftly increase afterwards. At 99% water content, the emission intensity is more than 4-fold higher than that in pure THF solution (Fig. 1). Since TPE-Py is insoluble in water, its molecules must have been aggregated in aqueous mixtures with high water contents. Evidently, TPE-Py is AIE-active. The formation of aggregates has activated the RIR process, thus making the dye more emissive in the aggregated state. However, the gradual addition of water into the THF solution has increased the polarity of the solvent mixture, which has intensified the ICT effect and hence weakened the light emission. The ICT effect seems to be dominated at water fraction ≤90%. Afterwards, the AIE process prevails, which converts TPE-Py into a strong emitter. It is noteworthy that the aggregates suspended in the aqueous mixture emit bluer color than their isolated species in THF solution because of the reduction in the solvent effect on their photophysical properties.

Interestingly, the emission intensity and color of a freshly prepared 95% aqueous mixture change when standing at room temperature with time. As depicted in Fig. 2A, the emission peak at 600 nm becomes weaker progressively as time elapses. Meanwhile, a new peak with enhanced intensity appears at 512 nm. After 30 min, the peak at 600 nm disappears completely and the emission spectrum is dominated by the peak at 512 nm. At the same time, the emission color changes from yellow to green under 365 nm UV irradiation, as suggested by the photographs shown in the inset of Fig. 2B. Similar observation was found in 90% aqueous mixture, though the time to reach

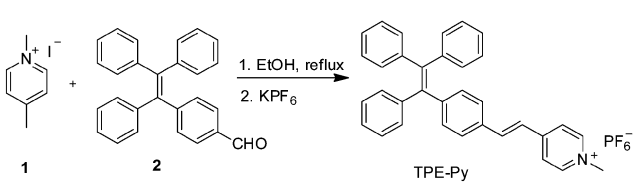

Scheme 1 Synthetic route to TPE-Py.

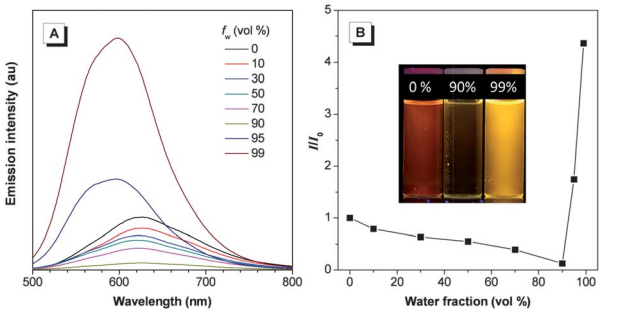

Fig. 1 (A) Emission spectra of TPE-Py in THF–water mixtures with different water fractions (f_w). Solution concentration: 20 μM; excitation wavelength: 403 nm. (B) Plot of the relative emission intensity (I/I_0) *versus* the composition of the aqueous mixture of TPE-Py. I_0 = emission intensity in pure THF solution. Inset in (B): photographs of TPE-Py in THF–water mixtures with f_w values of 0, 90 and 99% taken under 365 nm UV irradiation.

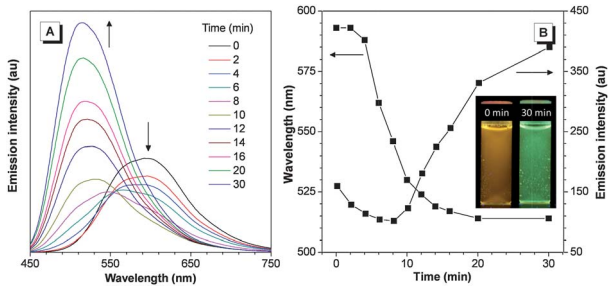

Fig. 2 Change in the emission spectrum of TPE-Py in 95% aqueous mixture with standing time at room temperature. Solution concentration: 20 μM; excitation wavelength: 403 nm. (B) Plot of wavelength and emission intensity *versus* the standing time from 0 to 30 min. Inset in (B): photographs of TPE-Py in 95% aqueous mixture taken at 0 and 30 min under 365 nm UV illumination.

equilibrium and the extent of emission enhancement are different (Fig. S3†).

To decipher the mechanism of such a phenomenon, we analyzed the aggregates suspended in 95% and 90% aqueous mixtures by transmission electron microscopy (TEM) and electron diffraction (ED). The TEM image of a freshly prepared 95% aqueous mixture exhibits spherical nanoparticles with varied sizes (Fig. 3A). Only a diffuse halo was observed in the associated ED pattern (Fig. 3B), suggesting that the aggregates are amorphous in nature. However, entirely different results were obtained after the mixture was standing at room temperature for 30 min. Flaky aggregates, rather than nanoparticles, were observed in the TEM image (Fig. 3C). The aggregates are crystalline, as revealed by the numerous diffraction spots in the ED pattern. Evidently, crystallization leads to such emission color and intensity changes, which is exactly the same as that observed in our previous publication.[17] The aggregates formed in 90% aqueous mixture are amorphous but crystalline when the mixture is left at room temperature for 135 min (Fig. S4†). Aqueous mixtures with water contents higher than 95% exhibit no such time-dependent phenomenon, probably due to the tighter packing of the formed aggregates, which hampers the reorientation and repacking of the TPE-Py molecules in a more ordered fashion. Crystallization generally red-shifts the emission spectrum and weakens the light emission. The unusual phenomenon observed here may be due to the more conformational twisting of the TPE-Py molecules in order to fit into the crystal lattice. The stronger interaction between the TPE-Py molecules in the crystal state may, on the other hand, stiffen the molecular conformation and hinder intra- and inter-molecular motions, thus making the crystalline aggregates stronger emitters.[19]

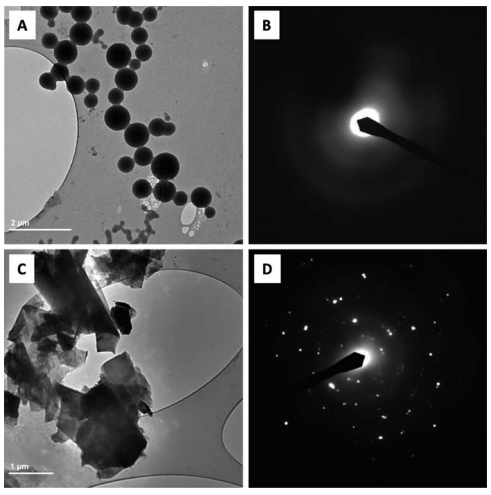

Fig. 3 (A and C) TEM images and (B and D) ED patterns of (A and B) amorphous and (C and D) crystalline aggregates of TPE-Py formed in 95% aqueous mixture (A and C) before and (B and D) after standing at room temperature for 30 min.

Mechanochromic luminescence

Mechanochromic luminophores are smart materials and show a sensitive response to external stimuli. They have received considerable attention in recent years for their potential applications in the optical information storage media and memory system.[20] Some AIE luminogens with good mechanochromic properties have been prepared in view of their facile transformation between the crystalline and amorphous states in response to external stimuli, the emission contrast, however, is low in most cases.[21] Since the amorphous and crystalline aggregates of TPE-Py exhibit different emission behaviours, it encourages us to investigate its mechanochromic property. Pale-yellow crystals of TPE-Py were readily obtained by slow evaporation of its dichloromethane (DCM)–hexane mixture at room temperature. Unfortunately, the sizes of the crystals are too small to be analysed by crystal X-ray diffraction. UV irradiation of the TPE-Py crystals gives a strong green emission at 515 nm with a Φ_F value of 31.8% (Fig. 4A). After gentle grinding the crystals using a metal spatula, yellow powders are formed. The powders emit at 600 nm, giving a large emission contrast of ~85 nm. At the same time, the Φ_F value drops to 20.4%. Such a transformation is reversible aided by fuming with acetone vapor for 10 min or heating at 150 °C for 10 min. The conversion between the green- and yellow-emissive solids as well as their

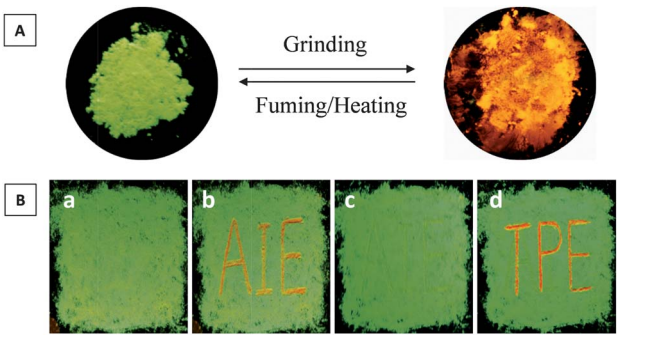

Fig. 4 (A) Switching the solid-state emission of TPE-Py by the grinding–fuming/heating process. (B) Fluorescent images of TPE-Py thin films on filter papers (a) without and (b) with letters of "AIE" being written by using a metal spatula. The photograph in (c) was obtained by fuming the film in (b) with acetone vapour for 10 min, while that in (d) was obtained by writing the letters of "TPE" on the TPE-Py film in (c) using a metal spatula. All the photos were taken under 365 nm UV irradiation.

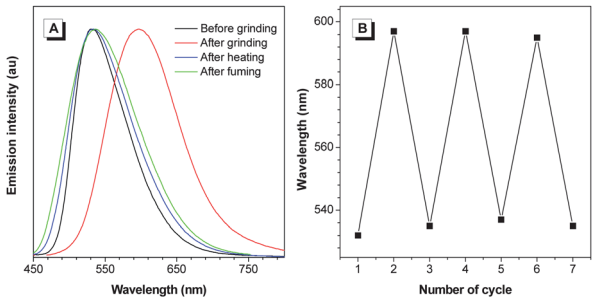

Fig. 5 (A) Change in the emission spectrum of TPE-Py crystals by the grinding–fuming/heating process. (B) Repeated switching of the solid-state fluorescence of TPE-Py by repeated grinding and fuming/heating cycles.

corresponding emission spectra can be repeated many times without fatigue because these external stimuli are non-destructive in nature (Fig. 5B).

To demonstrate their useful practical application, TPE-Py crystals were spread on a filter paper as a thin film (Fig. 4B). Under 365 nm UV irradiation, the TPE-Py film exhibits strong green emission. Letters of "AIE" are written on the film using a metal spatula, which appear yellow and thus can be readily discernible from the background due to their high contrast. Fuming the film with acetone vapour for 10 min erases the letters and reinstalls the original green background, allowing new letters of "TPE" to be written on the film using the same method. These results show that TPE-Py is potential to be used as a recyclable optical storage medium.

To prove that the same mechanism is responsible for the mechanochromism of TPE-Py, we analyzed TPE-Py in different aggregated states by powder X-ray diffraction (XRD). As shown in Fig. 6, the X-ray diffractogram of TPE-Py crystals shows many sharp diffraction peaks, which are indicative of their well-ordered structure. After grinding, almost all the diffraction peaks disappear, suggesting that the ground sample possesses low crystallinity or is even amorphous. When such a sample was thermal-treated or fumed by solvent vapor, sharp diffraction peaks emerge again due to the recrystallization of the TPE-Py molecules, though the spectral pattern is different from that of the untreated one.

Analysis by differential scanning colorimetry (DSC) also supports the above claim (Fig. 6B). The heating scan of the ground sample detects an exothermic peak at 139 °C. Since TPE-Py degrades at temperatures higher than 200 °C as revealed by the TGA analysis, the transition at 139 °C thus should not be due to the thermal decomposition of the dye molecule but is associated with its crystallization process. No signals are detected in untreated, thermal-annealed and fumed samples as they are in the crystalline state. Due to the propeller-like TPE unit, non-covalent interactions may only exist between the TPE-Py molecules, which can be readily destroyed in the presence of mechanical perturbation and recovered through thermal and solvent-fuming processes.

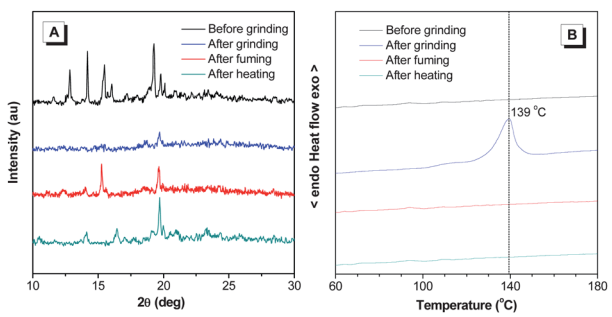

Fig. 6 (A) XRD diffractograms and (B) DSC thermograms of TPE-Py in different aggregated states recorded at a heating rate of 10 °C min^{-1}.

Optical waveguide

Development of organic crystals in the field of photoelectric material is a hot research topic for their well-ordered arrangement and high stability and mobility.[22] As crystalline AIE molecules show high solid-state emission, they are thus promising photoelectric materials. Indeed, a few micro/nano-crystalline AIE dyes have been fabricated and utilized as optical waveguide and amplified spontaneous light-emitting materials.[23] When observed under the fluorescent microscope, the crystalline microrods of TPE-Py formed by self-organization in the DCM–hexane mixture exhibit bright green emission (Fig. 7A). Careful investigation shows that the two ends emit more intensely, suggesting that TPE-Py exhibits optical waveguide behaviour.[22b,23b,24] To prove this, a distance-dependent fluorescent image of a single microrod was measured on a near-field scanning optical microscope. As shown in Fig. 7B, the chosen microrod on the glass coverslip is excited using a uniform focused laser (351 nm) at six different local positions

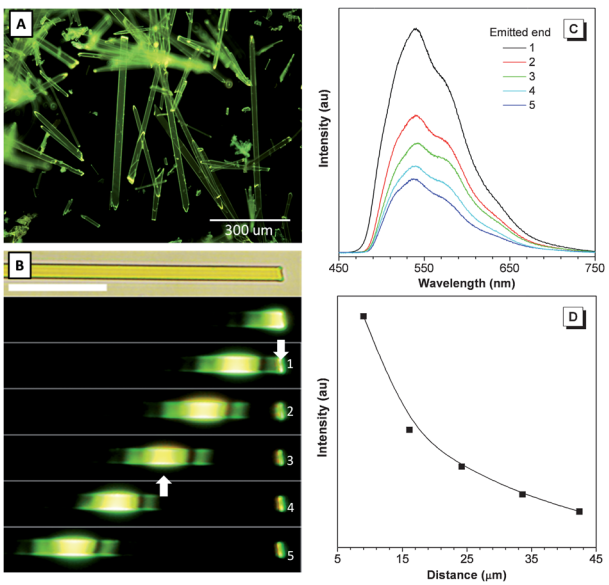

Fig. 7 (A) Fluorescent image of crystalline microrods of TPE-Py taken under UV irradiation on a fluorescent microscope. (B) Fluorescent micrographs obtained by exciting an identical TPE-Py microrod at different positions, where the up arrow indicated the excited site and the down arrow showed the emitted end. Scale bar: 20 μm. (C) Corresponding emission spectra of the emitted ends labelled with numbers 1–5 in (B). (D) Plot of emission intensity at the end *versus* the distance between the excited site and the emitted end.

along its length. Interestingly, except for the excited sites, green emission was also observed at both ends (since the microrod is long, only ends labelled with numbers 1–5 are shown). This phenomenon may originate from the absorption of the excitation light by TPE-Py molecules and propagation of the light emission to the rod end. Clearly, the appearance of outcoupling light demonstrates the strong waveguide property. Thus, according to previous reports, TPE-Py can be classified as active waveguide materials as the light is generated from the light emission process.[22b]

The corresponding emission spectra taken at varied excitation positions and fixed emitted ends are shown in Fig. 7C. By lengthening the distance between the excited site and the emitted end, the emission at the rod end becomes weaker due to the optical loss during the propagation process but causes no change in the spectral pattern. The optical loss coefficient (α) is an important parameter to determine the property of waveguide materials.[25] To determine the α value, the emission intensity at the fixed end (I_{end}) and the excited site (I_{body}) are recorded. By fitting the curve in Fig. 7D using a single exponential fitting, an equation in the form of $I_{end}/I_{body} = A\exp^{-\alpha x}$ was obtained,[25b] where x is the distance between the excited site and the emitted end and A is the ratio of the light that has escaped from the excitation spot and that of light propagated along the rod. Herein, the α value of TPE-Py is determined to be 0.032 dB μm^{-1}, which is quite low compared with the previous reported values.[23a,25a,26] The low optical loss coefficient of TPE-Py may be related to its intrinsic property of large Stokes shift, which helps decrease re-absorption. Moreover, the smooth surface and well-ordered molecular arrangement of the crystalline microrods, as suggested by powder X-ray diffraction, may also contribute to such good optical waveguide behaviour, which is rarely reported for TPE derivatives.

Mitochondrion staining

We also explored the utilization of TPE-Py as a fluorescent visualizer for intracellular imaging.[12,27] The nanoaggregates of TPE-Py were prepared in the minimum essential medium–dimethyl sulfoxide mixture and the HeLa cells were imaged using a standard cell-staining protocol. The living cells were incubated with TPE-Py (5 μM) for 15 min at 37 °C and then washed three times with phosphate buffered saline solution. As shown in Fig. S5,† the living cells grow healthy and display their normal morphology, demonstrating that TPE-Py is biocompatible. Amusingly, when investigated under a fluorescent microscope, distinct yellow emission likely originated from the mitochondria was observed.

To confirm the above speculation, we co-incubated the living cells with TPE-Py and MitoTracker Red CMXRos (100 nM), a widely utilized mitochondrion-targeted dye. We took fluorescent images of one cell stained by TPE-Py and MitoTracker Red, which show yellow and red emissions, respectively (Fig. 8A and B). Merging both photos generates an orange image, from which the position, shape and amount of mitochondria stained by TPE-Py are found to be the same as those by MitoTracker Red. Clearly, TPE-Py can specifically stain the mitochondria of living cells.

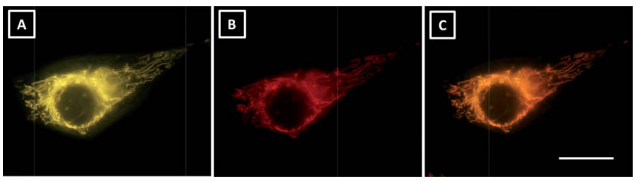

Fig. 8 Fluorescent images of a HeLa cell incubated with (A) TPE-Py (5 μM) and (B) MitoTracker Red (100 nM) for 15 min at 37 °C, and (C) their merged picture. Scale bar: 20 μm.

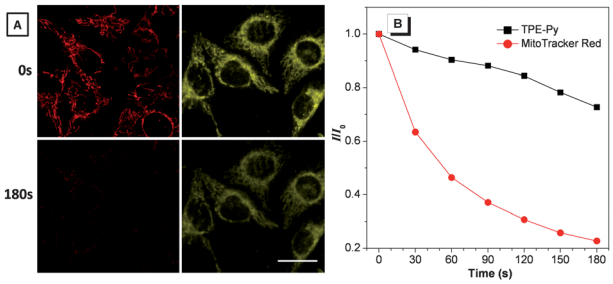

Fig. 9 (A) Fluorescent images of HeLa cells stained with TPE-Py and MitoTracker Red taken under continuous UV excitation at 405 nm and 560 nm, respectively, for 0 and 180 s. Scale bar: 20 μm. (B) Luminescence decay curves of TPE-Py and MitoTracker Red.

To work as a good intracellular visualizer, it should possess high resistance to photobleaching. With such regard, the photostability of TPE-Py as well as MitoTracker Red was examined under the same experimental conditions. After continuous excitation for 180 s, the emission from the living cells stained with MitoTracker Red is largely quenched (Fig. 9A). The measurement of the change in the emission intensity with time shows that the magnitude at 180 s is merely ~20% of the initial value owing to photobleaching (Fig. 9B). Amazingly, after continuous excitation at identical power for the same time, strong light was still observed in living cells incubated with TPE-Py as the emission intensity drops only 30% under such circumstances. Evidently, TPE-Py possesses a stronger photostability or higher resistance to photobleaching than MitoTracker Red.

It is well-known that a mitochondrion shows a large negative potential on the matrix side of the membrane. Thus, mitochondrion-targeted fluorescent dyes are generally lipophilic and cationic in character.[4,12b,28] TPE-Py possesses both such characteristics and thus makes it work as a good staining agent for specific targeting of mitochondrion in a living cell.

Conclusions

In summary, a heteroatom-containing luminogen with multifunctionality was synthesized in a reasonable yield by melding a pyridinium unit with TPE. Whereas TPE-Py is weakly emissive in solution, it becomes a strong emitter when aggregated, demonstrating a phenomenon of aggregation-induced emission. Crystallization generally weakens and red-shifts the light emission. The crystalline aggregates of TPE-Py, however, show stronger and bluer light than their amorphous aggregates. Its

solid-state emission can be reversibly switched between green and yellow color with a high contrast by grinding and fuming or heating processes due to the morphological change from the thermodynamically stable crystalline phase to the metastable amorphous state. Crystalline microrods of TPE-Py show an excellent optical waveguide property with low optical loss. Thanks to its cationic and lipophilic nature, TPE-Py works as a fluorescent visualizer for specific staining of mitochondria in living cells with high photostability. It is anticipated that the ready synthesis of TPE-Py coupled with its multi-potential applications will trigger new research enthusiasm and effort for the creation of new AIE materials with improved or new properties for more high-technological applications.

Acknowledgements

The work reported in this paper was partially supported by the National Basic Research Program of China (973 Program, 2013CB834701), the RPC and SRFI Grants of HKUST (RPC11SC09 and SRFI11SC03PG), the Research Grants Council of Hong Kong (HKUST2/CRF/10 and N_HKUST620/11), and the University Grants Committee of Hong Kong (AoE/P-03/08). B.Z.T. thanks the support of the Guangdong innovative Research Team Program (201101C0105067115).

Notes and references

1 (*a*) L. Xiao, Z. Chen, B. Qu, J. Luo, S. Kong, Q. Gong and J. Kido, *Adv. Mater.*, 2011, **23**, 926; (*b*) H. Xia, D. Liu, K. Song and Q. Miao, *Chem. Sci.*, 2011, **2**, 2402.

2 C. Zhang, Y. Yan, Y.-Y. Jing, Q. Shi, Y. S. Zhao and J. Yao, *Adv. Mater.*, 2012, **24**, 1703.

3 M.-J. Teng, X.-R. Jia, S. Yang, X.-F. Chen and Y. Wei, *Adv. Mater.*, 2012, **24**, 1255.

4 E. De Meulenaere, W.-Q. Chen, S. Van Cleuvenbergen, M.-L. Zheng, S. Psilodimitrakopoulos, R. Paesen, J.-M. Taymans, M. Ameloot, J. Vanderleyden, P. Loza-Alvarez, X.-M. Duan and K. Clays, *Chem. Sci.*, 2012, **3**, 984.

5 (*a*) A. C. Grimsdale, K. Leok Chan, R. E. Martin, P. G. Jokisz and A. B. Holmes, *Chem. Rev.*, 2009, **109**, 897; (*b*) J. Liu, J. W. Y. Lam and B. Z. Tang, *Chem. Rev.*, 2009, **109**, 5799.

6 J. Luo, Z. Xie, J. W. Y. Lam, L. Cheng, H. Chen, C. Qiu, H. S. Kwok, X. Zhan, Y. Liu, D. Zhu and B. Z. Tang, *Chem. Commun.*, 2001, 1740.

7 J. Chen, C. C. W. Law, J. W. Y. Lam, Y. Dong, S. M. F. Lo, I. D. Williams, D. Zhu and B. Z. Tang, *Chem. Mater.*, 2003, **15**, 1535.

8 (*a*) Y. Hong, J. W. Y. Lam and B. Z. Tang, *Chem. Soc. Rev.*, 2011, **40**, 5361; (*b*) Y. N. Hong, J. W. Y. Lam and B. Z. Tang, *Chem. Commun.*, 2009, 4332.

9 (*a*) Z. J. Zhao, S. M. Chen, J. W. Y. Lam, Z. M. Wang, P. Lu, F. Mahtab, H. H. Y. Sung, I. D. Williams, Y. G. Ma, H. S. Kwok and B. Z. Tang, *J. Mater. Chem.*, 2011, **21**, 7210; (*b*) Z. J. Zhao, J. L. Geng, Z. F. Chang, S. M. Chen, C. M. Deng, T. Jiang, W. Qin, J. W. Y. Lam, H. S. Kwok, H. Y. Qiu, B. Liu and B. Z. Tang, *J. Mater. Chem.*, 2012, **22**, 11018; (*c*) J. Huang, X. Yang, J. Wang, C. Zhong, L. Wang, J. Qin and Z. Li, *J. Mater. Chem.*, 2012, **22**, 2478; (*d*) J. Huang, N. Sun, J. Yang, R. Tang, Q. Li, D. Ma, J. Qin and Z. Li, *J. Mater. Chem.*, 2012, **22**, 12001.

10 H. Shi, J. Liu, J. Geng, B. Z. Tang and B. Liu, *J. Am. Chem. Soc.*, 2012, **134**, 9569.

11 (*a*) Y. Liu, Y. H. Tang, N. N. Barashkov, I. S. Irgibaeva, J. W. Y. Lam, R. R. Hu, D. Birimzhanova, Y. Yu and B. Z. Tang, *J. Am.Chem. Soc.*, 2010, **132**, 13951; (*b*) C. Y.-S. Chung and V. W.-W. Yam, *J. Am. Chem. Soc.*, 2011, **133**, 18775; (*c*) M. Wang, G. Zhang, D. Zhang, D. Zhu and B. Z. Tang, *J. Mater. Chem.*, 2010, **20**, 1858; (*d*) J. Wu, W. Liu, J. Ge, H. Zhang and P. Wang, *Chem. Soc. Rev.*, 2011, **40**, 3483; (*e*) C. Li, T. Wu, C. Hong, G. Zhang and S. Liu, *Angew. Chem., Int. Ed.*, 2012, **51**, 455.

12 (*a*) C. W. T. Leung, Y. Hong, S. Chen, E. Zhao, J. W. Y. Lam and B. Z. Tang, *J. Am. Chem. Soc.*, 2012, **135**, 62; (*b*) Y. Yu, C. Feng, Y. Hong, J. Liu, S. Chen, K. M. Ng, K. Q. Luo and B. Z. Tang, *Adv. Mater.*, 2011, **23**, 3298; (*c*) H. Lu, F. Su, Q. Mei, Y. Tian, W. Tian, R. H. Johnson and D. R. Meldrum, *J. Mater. Chem.*, 2012, **22**, 9890.

13 (*a*) T. Han, X. Feng, B. Tong, J. Shi, L. Chen, J. Zhi and Y. Dong, *Chem. Commun.*, 2012, **48**, 416; (*b*) Z. Shi, J. Davies, S.-H. Jang, W. Kaminsky and A. K. Y. Jen, *Chem. Commun.*, 2012, **48**, 7880; (*c*) J. Liu, H. Su, L. Meng, Y. Zhao, C. Deng, J. C. Y. Ng, P. Lu, M. Faisal, J. W. Y. Lam, X. Huang, H. Wu, K. S. Wong and B. Z. Tang, *Chem. Sci.*, 2012, **3**, 2737; (*d*) J. Huang, N. Sun, J. Yang, R. Tang, Q. Li, D. Ma, J. Qin and Z. Li, *J. Mater. Chem.*, 2012, **22**, 12001; (*e*) N. B. Shustova, T.-C. Ong, A. F. Cozzolino, V. K. Michaelis, R. G. Griffin and M. Dincă, *J. Am. Chem. Soc.*, 2012, **134**, 15061.

14 (*a*) Z. Guo, W. Zhu and H. Tian, *Chem. Commun.*, 2012, **48**, 6073; (*b*) X. Wang, A. R. Morales, T. Urakami, L. Zhang, M. V. Bondar, M. Komatsu and K. D. Belfield, *Bioconjugate Chem.*, 2011, **22**, 1438.

15 J.-A. Richard, M. Massonneau, P.-Y. Renard and A. Romieu, *Org. Lett.*, 2008, **10**, 4175.

16 (*a*) Z. R. Grabowski, K. Rotkiewicz and W. Rettig, *Chem. Rev.*, 2003, **103**, 3899; (*b*) R. R. Hu, E. Lager, A. Aguilar-Aguilar, J. Z. Liu, J. W. Y. Lam, H. H. Y. Sung, I. D. Williams, Y. C. Zhong, K. S. Wong, E. Pena-Cabrera and B. Z. Tang, *J. Phys. Chem. C*, 2009, **113**, 15845.

17 N. Zhao, Z. Yang, J. W. Y. Lam, H. H. Y. Sung, N. Xie, S. Chen, H. Su, M. Gao, I. D. Williams, K. S. Wong and B. Z. Tang, *Chem. Commun.*, 2012, **48**, 8637.

18 (*a*) J. Wang, J. Mei, R. R. Hu, J. Z. Sun, A. J. Qin and B. Z. Tang, *J. Am. Chem. Soc.*, 2012, **134**, 9956; (*b*) X. Zhang, Z. Chi, B. Xu, L. Jiang, X. Zhou, Y. Zhang, S. Liu and J. Xu, *Chem. Commun.*, 2012, **48**, 10895.

19 (*a*) Y. Dong, J. W. Y. Lam, A. Qin, J. Sun, J. Liu, Z. Li, J. Sun, H. H. Y. Sung, I. D. Williams, H. S. Kwok and B. Z. Tang, *Chem. Commun.*, 2007, 3255; (*b*) Z. Zhao, C. Y. K. Chan, S. Chen, C. Deng, J. W. Y. Lam, C. K. W. Jim, Y. Hong, P. Lu, Z. Chang, X. Chen, H. S. Kwok, H. Qiu and B. Z. Tang, *J. Mater. Chem.*, 2012, **22**, 4527.

20 (*a*) C. Weder, *J. Mater. Chem.*, 2011, **21**, 8235; (*b*) G. Q. Zhang, J. W. Lu, M. Sabat and C. L. Fraser, *J. Am. Chem. Soc.*, 2010, **132**, 2160.

21 (*a*) Z. Chi, X. Zhang, B. Xu, X. Zhou, C. Ma, Y. Zhang, S. Liu and J. Xu, *Chem. Soc. Rev.*, 2012, **41**, 3878; (*b*) X. Luo, J. Li, C. Li, L. Heng, Y. Q. Dong, Z. Liu, Z. Bo and B. Z. Tang, *Adv. Mater.*, 2011, **23**, 3261; (*c*) Y. Dong, B. Xu, J. Zhang, X. Tan, L. Wang, J. Chen, H. Lv, S. Wen, B. Li, L. Ye, B. Zou and W. Tian, *Angew. Chem., Int. Ed.*, 2012, **51**, 10782; (*d*) Z. Zhang, B. Xu, J. Su, L. Shen, Y. Xie and H. Tian, *Angew. Chem., Int. Ed.*, 2011, **50**, 11654; (*e*) S.-J. Yoon and S. Park, *J. Mater. Chem.*, 2011, **21**, 8338.

22 (*a*) D. Fichou, S. Delysse and J.-M. Nunzi, *Adv. Mater.*, 1997, **9**, 1178; (*b*) C. Zhang, Y. S. Zhao and J. Yao, *Phys. Chem. Chem. Phys.*, 2011, **13**, 9060.

23 (*a*) X. Gu, J. Yao, G. Zhang, Y. Yan, C. Zhang, Q. Peng, Q. Liao, Y. Wu, Z. Xu, Y. Zhao, H. Fu and D. Zhang, *Adv. Funct. Mater.*, 2012, **22**, 4862; (*b*) L. Heng, X. Wang, D. Tian, J. Zhai, B. Tang and L. Jiang, *Adv. Mater.*, 2010, **22**, 4716.

24 Q. H. Cui, Y. S. Zhao and J. Yao, *J. Mater. Chem.*, 2012, **22**, 4136.

25 (*a*) S. Chen, N. Chen, Y. L. Yan, T. Liu, Y. Yu, Y. Li, H. Liu, Y. S. Zhao and Y. Li, *Chem. Commun.*, 2012, **48**, 9011; (*b*) C. J. Barrelet, A. B. Greytak and C. M. Lieber, *Nano Lett.*, 2004, **4**, 1981.

26 C. Shi, Z. Guo, Y. Yan, S. Zhu, Y. Xie, Y. S. Zhao, W. Zhu and H. Tian, *ACS Appl. Mater. Interfaces*, 2013, **5**, 129.

27 W. Qin, D. Ding, J. Liu, W. Z. Yuan, Y. Hu, B. Liu and B. Z. Tang, *Adv. Funct. Mater.*, 2011, **22**, 771.

28 (*a*) X. Liu, Y. M. Sun, Y. H. Zhang, N. Zhao, H. S. Zhao, G. C. Wang, X. Q. Yu and H. Liu, *J. Fluoresc.*, 2011, **21**, 497; (*b*) G. Masanta, C. S. Lim, H. J. Kim, J. H. Han, H. M. Kim and B. R. Cho, *J. Am. Chem. Soc.*, 2011, **133**, 5698.

